



A Novel Multiscale Methodology for Simulating Tunnel Ventilation Flows During Fires

*Francesco Colella**, *Guillermo Rein* and *Jose L. Torero*, BRE Centre
for Fire Safety Engineering, University of Edinburgh, Edinburgh, UK
Romano Borchiellini, Dipartimento di Energetica, Politecnico di Torino,
Torino, Italy

Received: 11 September 2009/**Accepted:** 1 February 2010

Abstract. This paper applies a novel and fast modelling approach to simulate tunnel ventilation flows during fires. The complexity and high cost of full CFD models and the inaccuracies of simplistic zone or analytical models are avoided by efficiently combining mono-dimensional (1D) and CFD (3D) modelling techniques. A simple 1D network approach is used to model tunnel regions where the flow is fully developed (*far field*), and a detailed CFD representation is used where flow conditions require 3D resolution (*near field*). This multi-scale method has previously been applied to simulate tunnel ventilation systems including jet fans, vertical shafts and portals (Colella et al., Build Environ 44(12): 2357–2367, 2009) and it is applied here to include the effect of fire. Both direct and indirect coupling strategies are investigated and compared for steady state conditions. The methodology has been applied to a modern tunnel of 7 m diameter and 1.2 km in length. Different fire scenarios ranging from 10 MW to 100 MW are investigated with a variable number of operating jet fans. Comparison of cold flow cases with fire cases provides a quantification of the fire throttling effect, which is seen to be large and to reduce the flow by more than 30% for a 100 MW fire. Emphasis has been given to the discussion of the different coupling procedures and the control of the numerical error. Compared to the full CFD solution, the maximum flow field error can be reduced to less than few percents, but providing a reduction of two orders of magnitude in computational time. The much lower computational cost is of great engineering value, especially for parametric and sensitivity studies required in the design or assessment of ventilation and fire safety systems.

Keywords: Tunnel, Ventilation systems, Multiscale modelling, CFD, Jet fans

Nomenclature

a, b, c	Fan characteristic curve coefficients
c_p	Air specific heat [kJ/kg K]
D_h	Hydraulic diameter [m]
D_f	Diameter of the fire source [m]
f	Major losses coefficient

* Correspondence should be addressed to: Francesco Colella, E-mail: f.colella@ed.ac.uk
Francesco Colella, Dipartimento di Energetica, Politecnico di Torino, Torino, Italy.

G	Mass flow rate through a branch [kg/s]
G_{ext}	Mass flow rate exchanged with the external environment in a node [kg/s]
G_{g}	Mass flow rate of the gases released from the fire source [kg/m ³]
g	Gravity acceleration [m/s ²]
h	Convective heat transfer coefficient [W/m ² K]
L	Branch length [m]
L_{D}	Distance from the fan/fire region to the downstream boundary interface [m]
L_{CFD}	Length of the CFD domain in the multi-scale representation [m]
p	Pressure [Pa]
P	Branch perimeter [m]
Pr	Prandtl number
R	Wall-lining thermal resistance [K m ² /W]
T	Temperature [K]
T_{ext}	External environment temperature [K]
T_{g}	Temperature of the gases released from the fire source [K]
U	Overall heat transfer coefficient [W/m ² K]
v	Flow velocity [m/s]
z	Node elevation [m]
β	Minor losses coefficient
θ	Generic flow quantity [temperature or velocity]
ε	Average error of the multiscale model [%]
Φ	Fire heat release rate [W]
Φ^*	Dimensionless fire heat release rate
φ_{c}	Convective fire heat release rate per unit length [W/m]
λ	Flame radiative fraction
ρ	Air density [kg/m ³]
ρ_{ext}	Air density at external environment [kg/m ³]
Δp_{fan}	Pressure gain induced by jet fan [Pa]
Δp_{loss}	Pressure losses due to friction [Pa]

1. Introduction

In the past decade over four hundred people worldwide have died as a result of fires in road, rail and metro tunnels. In Europe alone, fires in tunnels have destroyed over a hundred vehicles, brought vital parts of the road network to a standstill—in some instances for years—and have cost the European economy billions of euros [1]. Disasters like the Mont Blanc tunnel fire (Italy–France, 1999) and the more three Channel Tunnel fires (2008, 2006 and 1996) show that fire events within tunnels should be managed by a global system capable of integrating detection, ventilation and fire fighting strategies in order to facilitate evacuation of occupants, assist the fire service and minimise damage to the structure. The ventilation system, installed in most tunnels, plays a crucial role controlling the smoke and maintaining acceptable conditions within the tunnel during evacuation, rescue and fire fighting procedures. The response of the ventilation system during a fire is a complex problem. The resulting air flow within a tunnel is dependent on the combination of the fire-induced flows and the active ventilation devices (jet fans, axial fans), tunnel layout, atmospheric conditions at the portals and the presence of vehicles. Depending on the accuracy required and the resources available, a solution to the problem can be reached using different numerical tools.

The overall behaviour of the ventilation system can be approximated using 1D fluid dynamics models under the assumptions that all the fluid-dynamic quantities are effectively uniform in each tunnel cross section and gradients are only present in the longitudinal direction. 1D models have low computational requirements and are specially attractive for parametric studies where a large number of simulations have to be conducted. In the last two decades several contributions on the application of 1D models to tunnel flows have been published. Ferro et al. [2] presented a 1D computer model for tunnel ventilation. The model was designed to deal with complex tunnel network including phenomena like piston effect and evolution of pollutant concentration. The calculations were performed in steady state and without fire. The same theoretical approach was used in the contribution by Jacques [3] presenting a numerical simulation of a complex urban tunnel longer than 2.5 km.

More recent applications of this methodology to real tunnels were presented by Riess et al. [4] and Cheng et al. [5]. The model presented by Riess and co-workers was tested on experimental data gathered from real tunnels whose length ranged between 0.8 km and 11 km. The model presented by Cheng and co-workers was tested on experimental data from a small scale underground transportation system and then applied to simulate a hypothetical fire outbreak in the Taipei Mass Rapid Transit System. Jang and Chen [6] provided also a methodology to estimate the aerodynamic coefficients of a 1.7 km long road tunnel using numerical modelling and experimental measurements. All the previous contributions underline the strength of 1D models to investigate ventilation scenarios within tunnels. However, this modelling approach cannot predict the characteristics of complex three-dimensional (3D) flow regions typically encountered close to operating ventilation devices (jet fans), intersection of galleries (shafts) or close to the fire, where air entrainment, plume formation and thermal stratification dominate the flow movement. Thus, in order to account for these important elements, 1D models must rely on approximated overall aerodynamics coefficients calculated somewhere else [6].

Several applications of 1D modelling of fire events in tunnels have been also proposed by Institutions including CETU and U.S. Department of Transportation. Among the calculation codes there are: SPRINT [4], MFIRE [5], ROAD-TUN [7] and SES [8].

Computational fluid dynamics (CFD) remains the most powerful method to predict the flow behaviour due to ventilation devices, large obstructions or fire but its use requires much larger computational resources than simpler 1D models. In the last two decades, the application of CFD as a predictive tool for fire safety engineering has become widespread. The results are still limited due to the difficulties of modelling turbulence, combustion, buoyancy and radiation in large enclosures [9] but great achievements have been made. Woodburn and Britter [10, 11] performed a CFD study of a 360 m long longitudinally ventilated tunnel and the numerical results agreed well with the experimental measurements. Wu and Bakar [12], Vaquelin and Wu [13] and Van Maele and Merci [14] used CFD tools to calculate the critical velocity and its dependency on the tunnel width. The experiments were conducted in a 15 m long small scale tunnel. All the previous works confirmed the capability of CFD tool as instrument to predict the critical velocity.

Only a limited number of CFD studies directly focuses on the performance of tunnel ventilation systems like jet fans or axial fans. This kind of analysis usually requires the adoption of a very large computational domain including the tunnel regions where the operating ventilation devices are located. Armstrong [15] and Tabarra [16] studied the flow generated by fans in a rectangular tunnel. Both of these works dealt with cold flow and resulted in a good agreement between experimental and numerical measurements. Karki and Patankar [17] described an application of CFD to simulate ventilation flows during a fire. The model has been previously validated using the 1995 Memorial Tunnel tests [18] and showed an acceptable agreement with the experimental measurements in the far-field of the domain. The agreement is not favourable in the vicinity of the fire. The Memorial Tunnel tests [18] have also been used by Galdo Vega [19] to validate a CFD model which included ventilation devices (jet fans).

CFD analysis of fire phenomena within tunnels suffers from the limitations set by the size of the computational domains. The high aspect ratio between longitudinal and transversal length scales leads to very large meshes. The number of grid points escalates with the tunnel length and often becomes impractical for engineering purposes, even for short tunnels domains less than 500 m long. An assessment of the mesh requirements for tunnel flows is made by Colella et al. [20] for active ventilation devices and no fire and by Van Maele and Merci [14] for fire-induced flows without active ventilation devices.

The high computational cost leads to the practical problem that arises when the CFD model has to consider boundary conditions or flow characteristics in locations far away from the region of interest. This is the case of tunnel portals, ventilation stations or jet fan series located long distances away from the fire. In these cases, even if only a limited region of the tunnel has to be investigated for the fire, an accurate solution of the flow movement requires that the numerical model includes all the active ventilation devices and the whole tunnel layout. For typical tunnels, this could mean that the computational domain is several kilometres long.

2. Multiscale Model

The study of ventilation and fire-induced flows in tunnels [12–14, 17, 19, 20] provides the evidence that in the vicinity of operating jet fans or close to the fire source the flow field has a complex 3D behaviour with large transversal and longitudinal temperature and velocity gradients. The flow in these regions needs to be calculated using CFD tools since any other simpler approach would only lead to inaccurate results. These regions are hereafter named as the *near field* [20]. However, it has been demonstrated for cold flow scenarios [20] and for fire scenarios [14] that at some distance downstream of these regions, temperature and velocity gradients in the transversal direction tend to disappear and the flow becomes 1D. In this portion of the domain the transversal components of the flow velocity can be up to two orders of magnitude smaller than the longitudinal components. These regions are hereafter named as the *far field* [20]. The use of CFD models to

simulate the fluid behaviour in the far field leads to large increases in the computational requirements but very small improvements in the accuracy of the results.

The adoption of multiscale models represents a way to avoid the large computational cost of the full CFD and the inaccuracies of simplistic assumptions of 1D models. A multiscale method uses different levels of detail when describing the fluid dynamic behaviour of near field and far field. The behaviour of far field and near field regions is modelled by using a 1D model and CFD model, respectively. The 1D and the CFD models exchange information at the 1D–3D interfaces and thus run in parallel.

This approach allows a significant reduction of the computational time. At the moment multiscale modelling techniques have been applied to design tunnel ventilation systems in no-fire operating conditions [20]. The application of multiscale techniques coupling the fire to the ventilations systems is the subject of this paper. For sake of simplicity and given the uncertainties related to transient phenomena during a tunnel fire (fire growth, decay phase, and delay time of the ventilation devices) only steady state calculations are discussed here. Nevertheless, the same multiscale methodology can be applied to perform transient simulations but this is out of the scope of the work.

In this work, the prediction capabilities of full CFD and multiscale models are compared in terms of accuracy and computational time using a modern tunnel as case study.

2.1. Mono-Dimensional Model of the Far Field

The general methodology of the 1D network model for tunnels is presented in [2, 20] and only an overview is given here. The first step is to generate a network of elements representing the tunnel layout. The longitudinal domain is discretised in oriented elements called branches, interconnected by nodes. The nodes are volume-less elements connecting different branches. Each node is characterized by vertical elevation and by the value of mass flow rate exchanged with the ambient (leaving or entering the domain). Pressures, densities and temperatures are defined in each node. The branches are oriented elements connecting two nodes. The characteristics of each branch are section, perimeter, length, wall roughness, coefficient for minor losses and pressure gain due to fan action. Velocities and mass flow rates are defined in each branch.

The model solves the mass conservation equation at each node and the momentum conservation equation across each branch. These governing equations are expressed for steady state and incompressible flow. An example of a general network layout is presented in Figure 1 where the nodes are numbered as i and branches as j . The mass conservation equation states that for each node the mass flow rate added or subtracted by connected branches has to be equal to the mass flow rate exchanged in the node with the external ambient

$$\sum_j G_j = G_{\text{ext},i} \quad (1)$$

where the summation is extended to all the branches j connected to the node i .

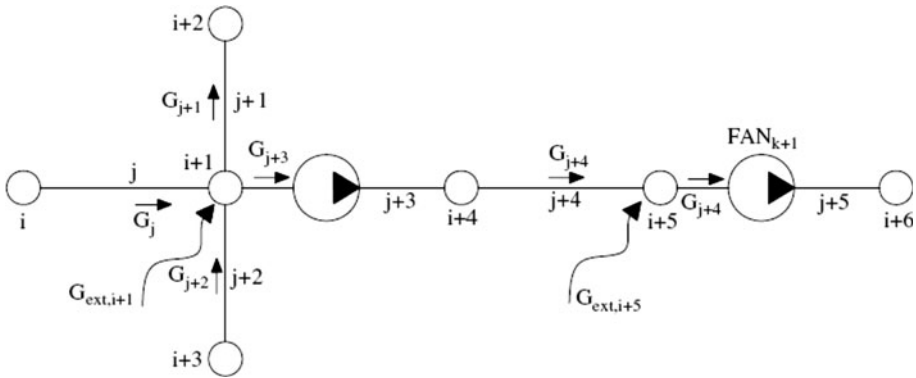


Figure 1. Example of the network representation of a tunnel showing branches between nodes.

The momentum conservation equation is written for each branch following the Bernoulli formulation. Given a branch j , between nodes i and $i + 1$, the longitudinal momentum equation states

$$p_{i+1} - p_i = \Delta p_j = -\Delta p_{\text{fan},j} - \bar{\rho}_j \left(\frac{v_{i+1}^2 - v_i^2}{2} \right) - \bar{\rho}_j g(z_{i+1} - z_i) - \Delta p_{\text{loss},j} \quad (2)$$

The pressure loss due to wall friction (major losses) and blockages (minor losses) is correlated to the flow velocity through the branch as [2–6]:

$$\Delta p_{\text{loss},j} = \bar{\rho}_j \cdot \frac{v_j^2}{2} \left(\frac{L_j}{D_{h,j}} f_j + \beta_j \right) \quad (3)$$

where the friction coefficient is computed using the Colebrook formula [21].

The pressure gain due to a fan inside the branch, also called the fan characteristic curve, is a function of the flow velocity through the branch and can be represented in general as a polynomial of second order [2–6] as

$$\Delta p_{\text{fan},j} = a + b \cdot v_j + c \cdot v_j^2 \quad (4)$$

In most cases, the fan characteristic curve is unknown or not well quantified because the fan behaviour is strongly coupled with the surrounding tunnel galleries and thus is dependent on installation details [6]. The jet fan thrust curve provided by a manufacturer only applies to the isolated jet fan and it does not describe its behaviour once installed in a particular tunnel gallery. Usually, in situ measurements or further CFD analysis are required to quantify accurately the fan characteristic curve (see [20] for an example in a real modern tunnel).

Temperature calculations require the solution of the energy conservation equation. Applying the energy conservation equation on a tunnel portion of length dx

where energy can be generated due to the fire ϕ_c or lost due to the heat transfer to the tunnel walls $UP(T - T_{\text{ext}})$, the following expression can be obtained:

$$Gc_p \frac{dT}{dx} = \phi_c - UP(T - T_{\text{ext}}) \quad (5)$$

The global heat transfer coefficient U is calculated as

$$U = \left(\frac{1}{h} + R \right)^{-1} \quad (6)$$

The Reynolds analogy [21], which is valid for Prandtl number close to 1, is considered as valid also for air (Pr equal to 0.7) and allows a good estimation of the convective heat transfer coefficient h as

$$h = \frac{1}{8} f c_p \rho v \quad (7)$$

The resulting Equation 5 is integrated along the length of each branch, producing an algebraic equation correlating inlet and outlet temperatures in the branch. The nodes are modelled as volume less elements where perfect mixing is assumed between the heat flow from branches and the heat flow from external ambient. Thus, the energy conservation equation for each node takes the form

$$\sum_j G_j c_p T_j = G_{\text{ext},i} c_p T_{i,\text{ext}} \quad (8)$$

where the summation on the LHS includes all the mass flow rate entering or leaving the node through a branch and the RHS represents the energy contribution carried by mass flow rate exchanged with the external ambient. The solution of the thermal problem in the whole 1D network can be achieved once energy conservation equations for branches and nodes are coupled together.

2.2. CFD Model of the Near Field

The CFD modelling of the near field has been conducted using the commercial CFD code FLUENT. This code has been extensively used for simulating duct flows and it has demonstrated its capability to model ventilation flows within tunnels as well as fire induced flows [12–14, 19, 20, 22].

The turbulent fluctuations of the fluid-dynamic quantities have been modelled by means of Reynolds-averaged Navier–stokes equations (RANS). Among all the RANS turbulence models, the $k-\varepsilon$ model has been applied in this work. The production and the destruction of turbulence kinetic due to the buoyancy have been also accounted for. RANS models have been extensively used and largely validated by the scientific community to simulate fire induced flows [10–14, 17, 19, 22, 23].

The standard $k-\varepsilon$ model is not valid for fluid regions characterized by low Reynolds numbers, like in locations close to walls [24]. In these regions the standard wall functions have been used providing adequate results for high Reynolds flows [25], and avoiding the need of high resolution meshes to solve the viscous sub-layer [26]. The wall function approach is valid as long as the first mesh point is located within the logarithmic region of the boundary layer. This constraint has been verified by means of a posteriori post-processing of the CFD results.

The fire has been modelled as a volumetric source of energy at a constant rate without using a dedicated combustion model. This simplified approach, previously used to model fire induced flows in tunnels [17, 19], is the most practical given its low computational cost. It avoids the burden and the complexity of combustion and radiation models and the large uncertainty associated to the burning of condensed-phase fuels. In particular the fire heat release rate (HRR), Φ , has been introduced in the computational domain as a rectangular slab releasing hot gases from the top surface simulating a burning vehicle. Mass conservation is applied by the extraction of air at the four lateral surfaces simulating air entrainment. For sake of generality the mass extraction from the lateral faces is uniform and independent from the ventilation conditions. This may not be completely true for high ventilation velocities but previous sensitivity studies have confirmed a minor impact of this modelling detail. The amount of gases injected into the domain is calculated using Equation 9 which correlates the convective HRR, $\Phi(1 - \lambda)$, to the temperature difference between air and hot gases:

$$G_g = \frac{\Phi(1 - \lambda)}{c_p(T_g - T_{ext})} \quad (9)$$

The flame radiative fraction λ can be up to 50% [27] but most measured values are around 35% (value used in this work). The main limitation of this approach is that the maximum flame temperatures are not accurate close to the fire source. However, as demonstrated by Vega et al. [19] and by Karki and Patankar [17], this methodology produces a good agreement with experimental temperature measurements of away from the flames. There is little information in the literature on the gas phase temperature in a tunnel close to the fire and its dependence on the ventilation conditions and fire size. Some experimental data are reported in the Runehamar tests in Norway [28], where the measured gas temperature above the centre of fire ranged between 1100 K and 1500 K. The same temperature range has been considered in this paper and the corresponding sensitivity of the solution investigated.

This modelling approach requires the definition of the top slab surface dimensions and its dependence on the fire size. A surface too small would bring unrealistic air behaviour given the corresponding excessively high inlet velocity for the hot gases and the wrong balance between the momentum and buoyancy of the fire source. Thus, the Froude number Φ^* is used here to link HRR and size of the fire source [29], defined as

$$\Phi^* = \frac{\Phi}{\rho_{\text{ext}} c_p T_{\text{ext}} D_f^2 \sqrt{g D_f}} \quad (10)$$

where D_f is the characteristic dimension of the fire source (hydraulic diameter of the slab top surface). Values of Φ^* above 2.5 are not realistic for diffusion flames [27]. Hence, the dimension of the fire source is calculated setting Equation 10 equal to 1, indicating a regime where the momentum and buoyancy strengths are of the same order. This choice is supported by the fact that typical tunnel fires can be represented as crib fires [30, 31] that, following [32], have Froude number in the range of 1. Future sensitivity studies can provide useful additional information, but they are out of the scope of this paper, which focuses only on the description of the multiscale methodology. Furthermore, the latter is valid independently of the way the fire is defined.

Once defined Φ^* equal to 1, the resulting top surface areas are 4.5 m², 11 m², 16 m² and 27 m², respectively for the 10 MW, 30 MW, 50 MW and 100 MW fire scenarios.

The tunnel walls have been assumed as adiabatic. Other heat transfer boundary conditions to the walls could be used, but the adiabatic condition represents the worst case in terms of buoyancy strength, threat to people and damage to the structure [33].

The CFD model requires also a representation of the jet fans. Previous works on CFD of tunnel ventilation [17, 19] simulated the jet fans as a combination of discharge source and intake sink of momentum and mass. This kind of approach has not been used in this paper avoiding the discrepancies in energy, momentum and species conservations that are generated by uncoupling discharge source and intake sink. The methodology used here simulates the real construction of the jet fans as a cylindrical fluid region delimited by walls and containing an internal cross surface where a constant positive pressure jump is enforced. In order to accurately predict the thrust with this approach or any other, it is highly recommended to use experimental data for calibration or validation of the results. This approach has been implemented successfully to model jet fan installed in a real tunnel where the comparison with experimental flow measurements is excellent [20].

The simulations have been considered to be converged when the scaled residuals were lower than 10^{-5} with the exception of the energy equation where the maximum allowed value was 10^{-7} .

2.3. Coupling Strategies at the Interfaces

1D and the CFD domains exchange information at the 1D–3D interfaces (nodes i and $i + 1$ in Figure 2). The coupling can be conducted in two different ways; direct and indirect coupling.

In *Direct coupling*, the 1D model is embedded within the CFD model and they run iteratively together. The solution of the multiscale model requires a constant exchange of information during the solution procedure. Direct coupling is

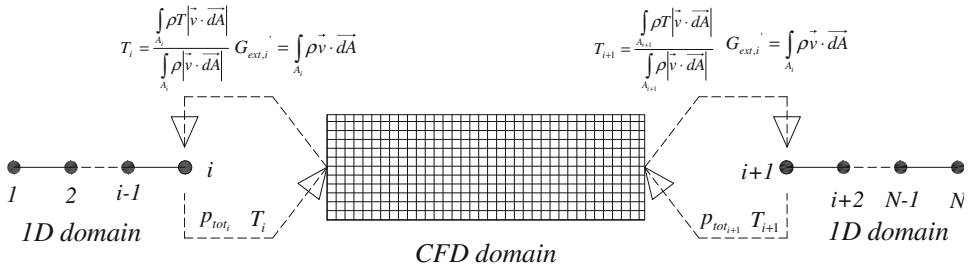


Figure 2. Boundary conditions exchange for the direct coupling of the 1D and CFD models.

required if details of the 3D flow field directly feedback to the 1D bulk flow, for example simulating the transient response of jet fans activation or rapid fire growth. The direct coupling algorithm has to perform the following operations at each iteration step:

1. provide the CFD model with the pressure and temperature boundary conditions at the interfaces i and $i + 1$ calculated by the 1D model
2. perform one iteration of the CFD model using a segregate solver
3. integrate the air velocities at the interfaces i and $i + 1$ to calculate the global mass flow rate and fix them as boundary for the 1D model (see Figure 2)
4. average the temperature at the interfaces i and $i + 1$ to provide the boundary conditions for the 1D model (see Figure 2)
5. solve the 1D model
6. repeat back to step 1 until convergence is reached.
7. proceed to the following time step (for transient calculations)

A more detailed overview of the sequence of operations required by the multi-scale model with direct coupling is presented in Figure 3.

However, for most ventilation studies, bulk flow velocities and average temperature values in steady state or quasi steady state conditions are needed. In this case an *indirect coupling* method can be adopted and 1D and CFD simulations would be run separately. After identifying the *near field*, a series of CFD runs has been conducted for a range of uniform boundary conditions at the interfaces. In this manner, the CFD results are arranged in terms of bulk flow velocities as a function of the total pressure differences across the *near field* allowing the definition of characteristic curves. These curves represent the coupling of the active element of interest (shaft, jet fan, or fire) with the surrounding tunnel gallery. The 1D model takes into account these curves, accurately calculated by the CFD model and, hence, it couples them to the rest of the tunnel.

Generally, direct coupling leads to longer computational times since the solving speed is set by the CFD model. Indirect coupling leads to higher set-up times, mainly on the calculation of the characteristic curves, but then provides almost instantaneous results of tunnel flows and temperatures.

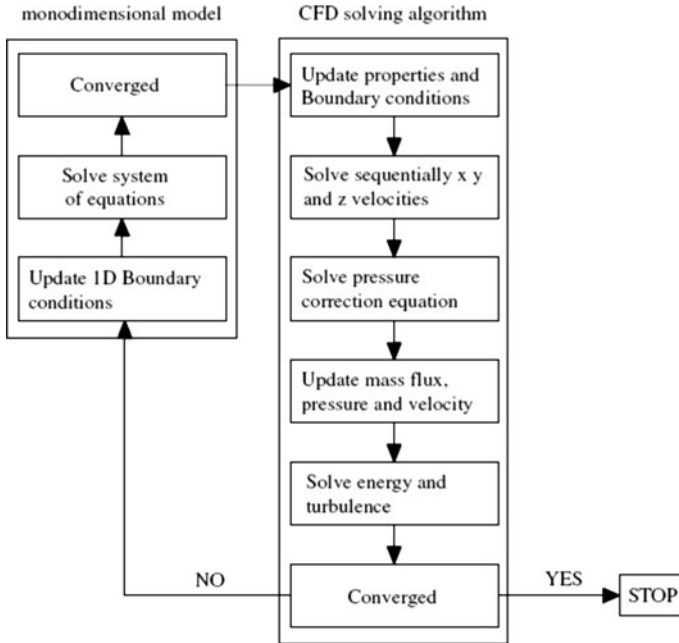


Figure 3. Solution algorithm for direct coupling of the 1D and CFD models.

Further considerations are required when dealing with the turbulent kinetic energy and the dissipation rate at the CFD domain boundaries. Since these quantities are not calculated by the 1D model, they are introduced as a function of turbulence intensity, turbulent length scale and Reynolds number using well known relations that can be found in the literature [24].

The 3D region must be sized appropriately, such that the boundary interfaces are located in regions where the flow is fully developed. In a previous work the effect of the multiscale interface location in the vicinity of an operating jet fan pair has been investigated [20]. It demonstrates that if the 1D–3D interface is located more than 150 m downstream the operating jet fans, the multiscale solution deviates from the full CFD solution by less than 1%. In this paper the effect of the interface location when modelling a tunnel fire is investigated and results presented in Sect. 3.2. In this paper both direct and indirect couplings have been used to model the behaviour of a longitudinal ventilated tunnel in normal operating conditions and in case of fire.

3. Case Study of a Modern Tunnel 1.2 km in Length

The previously discussed multiscale model has been used to simulate a 1200 m long tunnel longitudinally ventilated. This layout is realistic and typical of a

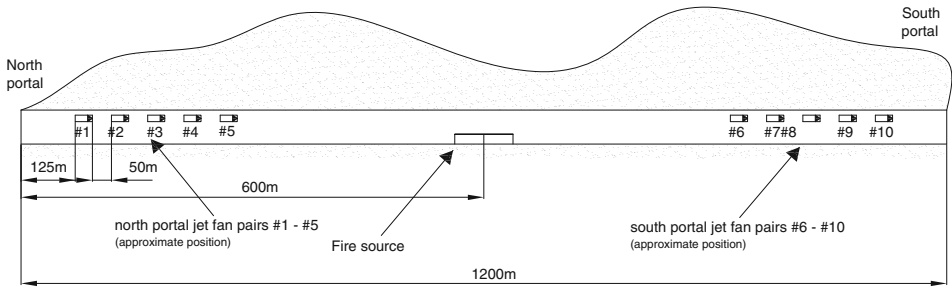


Figure 4. Layout of the tunnel used as case study showing the relative positions of the fire, jet fans and portals (Not to scale).

modern generic uni-directional road tunnel. A schematic of the tunnel layout is presented in Figure 4. The tunnel is 6.5 m high with a standard horseshoe cross section of around 53 m². The tunnel is equipped with two groups of five jet fans pairs spaced 50 m, each group installed near a tunnel portal. The jet fans are rated by the manufacturer at the volumetric flow rate of 8.9 m³/s with a discharge flow velocity of 34 m/s.

The fires are located in middle of the tunnel and four different sizes ranging from 10 MW to 100 MW are considered. The HRR is assumed to be constant and that steady state conditions are reached within the tunnel.

The emergency ventilation strategy, as for most longitudinally ventilated tunnels, requires the ventilation system to push all the smoke downstream from the incident region in the same direction as the road traffic flow, thus avoiding the smoke spreading against the ventilation flow (*back-layering effect*). The vehicles downstream the fire zone are assumed to leave the tunnel safely. All the studies on back layering show that the maximum critical velocity is in the range from 2.5 m/s to 3 m/s [12, 13, 34, 35]. Thus, an adequate ventilation system has to provide air velocities higher than this range in the region of the fire incident.

3.1. Grid Independence Study

The computational domain has been discretized using quasi structured meshes with refinements introduced close to each jet fan pairs and close to the fire source. Various full CFD runs of the whole tunnel domain have been conducted to estimate the mesh requirements. Four different meshes were generated and the resulting solutions compared. The mesh characteristics are resumed in Table 1. The symmetry of the solution across the longitudinal plane was also considered to reduce the computing time. Four examples of the mesh cross section are presented in Figure 5. The data presented are relative to a 30 MW fire scenario and ventilation conditions slightly above the critical velocity. This condition could be achieved by activating three jet fan pairs upstream the fire.

The solution is shown to converge as the mesh is made finer. A coarse mesh of 100 cells/m leads to a 15% underestimation of the average ventilation velocity. But a finer mesh of 2500 cells/m leads to results within 0.3% of the prediction

Table 1
Grid Independence Study of the Full CFD Domain for a 30 MW Fire and Three Operating Jet Fan Pairs

	Mesh density [cells/m]	Predicted air velocity [m/s]	Deviation from mesh 4 [%]
Mesh 1	105	3.21	-15.25
Mesh 2	695	3.83	0.98
Mesh 3	2525	3.80	0.32
Mesh 4	4125	3.79	-

made with the finest mesh. Besides the comparison of the average quantities, detailed field solutions have been compared at Reference Sections 1 and 2, located 10 m and 100 m downstream of the fire source, respectively. The location of these sections is shown in Figure 6. The comparison of the longitudinal velocity and temperature fields is plotted in Figure 7 for the Reference Section 1. For sake of simplicity the data relative to Reference Section 2 are presented in Appendix A.

As expected from the previous results, the computed solutions show larger deviations for the coarse meshes 1 and 2 while convergence of the temperature and velocity fields is obtained for finer meshes 3 and 4. Based on the results, grid independence is considered reached for mesh 3 and therefore, all the following simulations have been conducted using this mesh.

3.2. Boundary Independence Study

The downstream interface boundary between 1D and CFD domain must be located where the flow evolves to fully developed. Otherwise, the coupling would induce an error and the multiscale results would depend on the interface location. The previous paper on multiscale modelling of tunnel flows [20] provides the analysis of the effect of the interface location for cold flow scenarios. It shows that notable accuracy in the computed mass flow rate (error smaller than 1%) could be achieved when the ratio between L_d (distance from the fan to the downstream boundary interface) and D_h (tunnel hydraulic diameter) is around 20 [20].

In order to identify the boundary independence limit for cases including fire-induced flows, several runs of the multiscale model were conducted for a range of fire sizes. In each run the interface was placed progressively further downstream of the fire, increasing the longitudinal extension of the CFD domain L_{3D} (see Figure 6) and consequently reducing the extension of the 1D domain by the same amount. The position of the upstream interface between 1D and CFD domain is not as critical as the downstream one where the focus is put here, but for sake of generality the CFD domain is centered on the fire source. However, if the modeller is sure that during the simulated scenarios the ventilation velocity does not change direction and the air velocity is super-critical (therefore no back-layering occurs), the upstream boundary can be moved significantly closer to the fire. This would produce a further reduction of computing time.

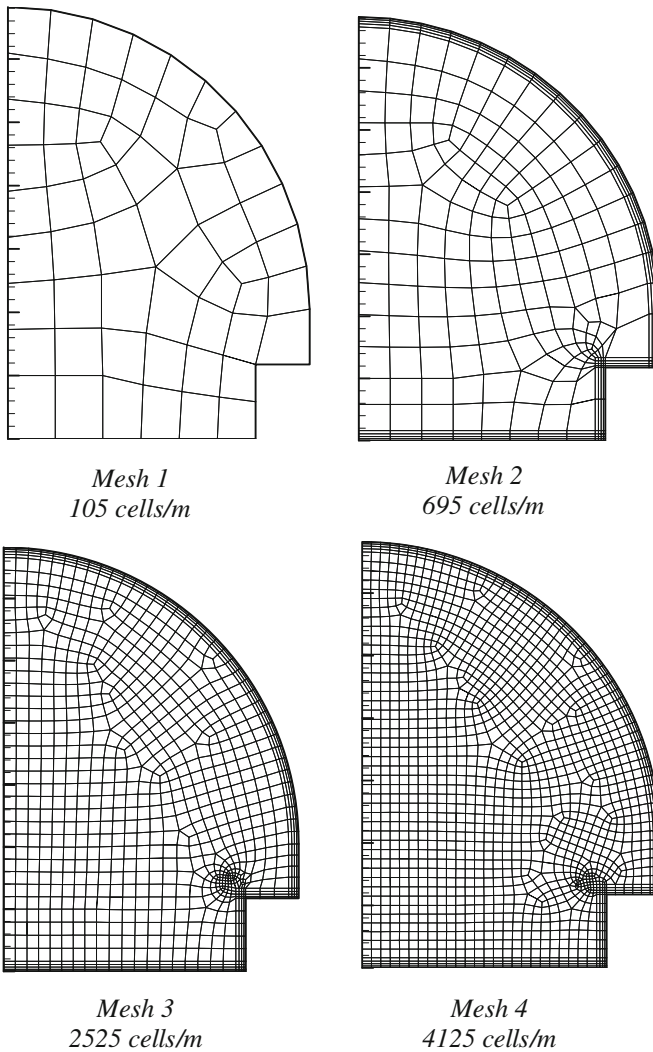


Figure 5. Examples of the different meshes used for half of the tunnel cross section and number of cells per unit length of tunnel.

In order to isolate the effect of the interface location on fire-induced flows, the jet fans at this stage are assumed to be located far away from the fire and thus simply modelled as a pressure difference between portals. This pressure difference is given by combining the characteristics curves of the operating fans.

A first analysis has been performed in order to clarify the dependence of the average bulk flow quantities (temperature and velocity) at the outlet boundary of the CFD domain. These values have an additional importance as they represent the input of the 1D model for the far field region located downstream the fire.

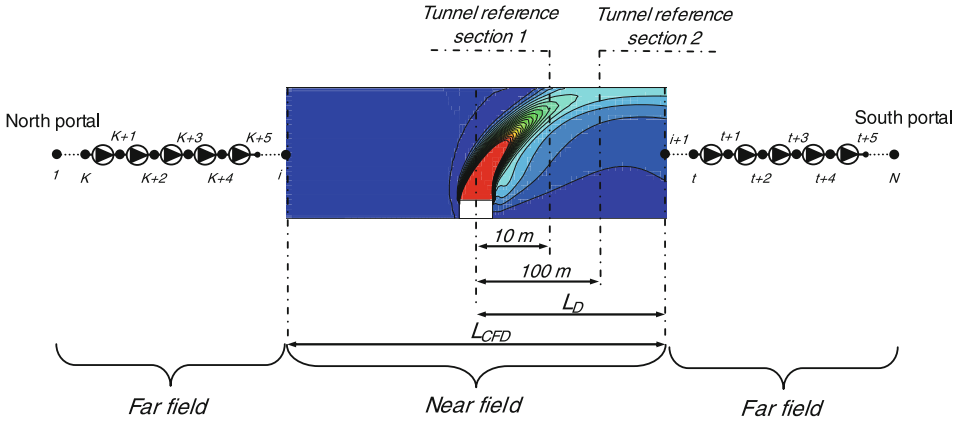


Figure 6. Schematic of the multiscale model of a 1.2 km tunnel including portals, jet fans, and the CFD domain of the fire region. Contours of the temperature field show the fire plume. (Not to scale).

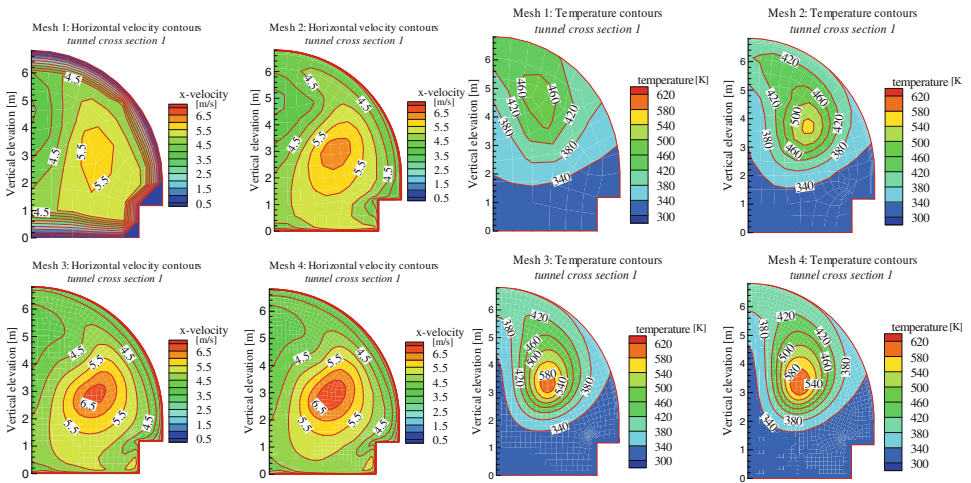


Figure 7. Comparison of the longitudinal velocity (left) and temperature (right) contours for meshes #1 to #4 in the tunnel at Reference Section 1 for a 30 MW fire. The velocity and temperature values are expressed in m/s and K, respectively.

Figure 8 represents the average velocities and temperatures (computed at the outlet of the CFD zone) for longitudinal dimensions of the CFD domain increasing from 20 m to 600 m. The points plotted for L_{CFD} equal to 1200 m are computed by using the full CFD model and represent the reference values in each scenario. It can be easily seen that, for CFD domain lengths between 20 m and 200 m, the

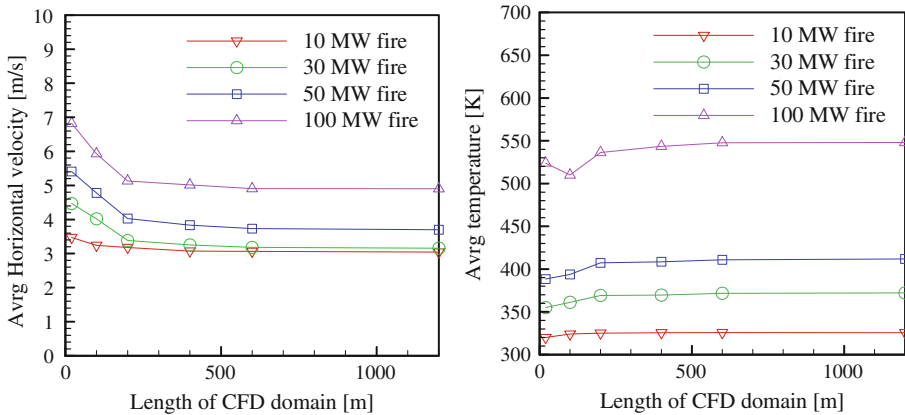


Figure 8. Effect of the CFD domain length, L_{CFD} , on the average longitudinal velocity and temperature at the outlet boundary of the CFD module. Units are in m/s and K, respectively. Note that the shortest module length is 20 m.

deviations in the average velocity from the reference values range between 6.5% and 40%; temperature variations range between 14% and 21%. No appreciable variations can be observed when the CFD domain length is larger than 200 m.

A second study has been performed in order to identify the dependence of the local flow field solutions on the dimension of the CFD domain. Also in this case, the full CFD data have been taken as reference solution. For a generic flow quantity ϑ , the associated average error has been calculated with the following norm

$$\varepsilon_{\vartheta} = \frac{\sum_{j=1}^N |\vartheta_{j,CFD} - \vartheta_{j,ms}|}{N \overline{\vartheta}_{CFD}} \quad (11)$$

where $\overline{\vartheta}_{CFD}$ is the average predicted by the full CFD simulation, and $\vartheta_{j,CFD}$ and $\vartheta_{j,ms}$ are the values calculated in each grid point j belonging to the Reference Section of interest. The subscripts CFD and ms are referred to the full CFD and multiscale simulation results. The summation over j is extended to all the N grid points belonging to the specific Reference Section.

The effect of the interface location on average values has been studied for four different fire sizes (10 MW, 30 MW, 50 MW and 100 MW) and presented in Figure 9. The results show that the error does not depend significantly on the dimension of the fire within that range. Figure 10 presents the field results at Reference Section 1 (See Appendix B for field results at Reference Section 2). The solution for a 20 m long domain provides low accuracy (15% error). The results become boundary independent and provide less than 1% error for domain lengths larger than 200 m (for Reference Section 1 at 10 m downstream of the fire source) and than 400 m (for Reference Section 2 at 100 m downstream of the fire source),

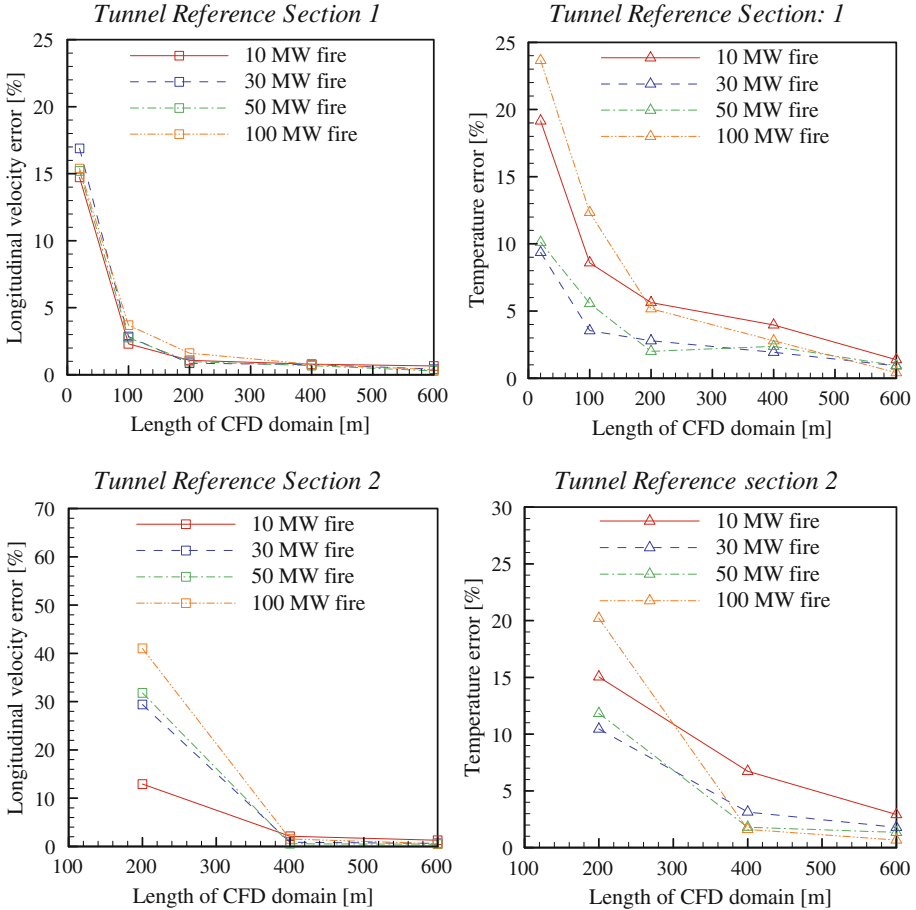


Figure 9. Effect of the CFD domain length L_{CFD} on the error for the average longitudinal velocity and average temperature. Results for top) Reference Section 1; bottom) Reference Section 2. Error calculated using Equation 11.

respectively. Thus, highly accurate results can be achieved with domains whose downstream boundary is at a minimum distance of 100 m from the furthest location where a CFD accurate solution is required.

In terms of the distance from the fire to the downstream boundary interface L_D (see Figure 6), the minimum ratio between L_D and the tunnel hydraulic diameter D_H is around 13. In a previous work Van Maele and Merci [14] simulated two different fire scenarios (3 kW and 30 kW) in a small scale tunnel ($0.25 \times 0.25 \text{ m}^2$ cross section) under ventilation conditions close to the critical velocity. The CFD solution in the vicinity of the fire plume became independent from the boundary location if the distance L_D was at least 12 times the hydraulic diameter. The agreement between the present and previous result is excellent.

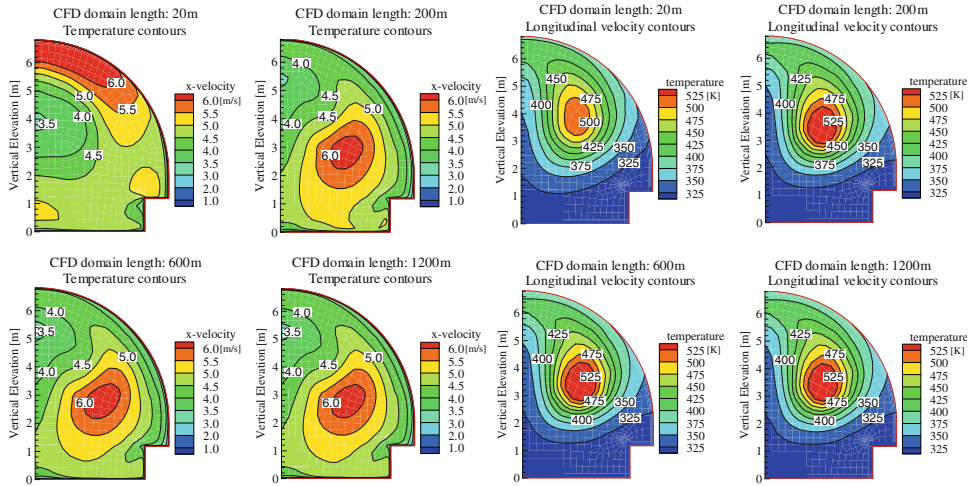


Figure 10. Effect of the CFD domain length L_{CFD} on the horizontal velocity and temperature fields at Reference Section 1 for a 30 MW fire. The velocity and temperature values are expressed in m/s and K, respectively.

Combining Figures 8, 9, and 10 allows identifying a range of module lengths between 20 m and 200 m where the average quantities at the outlet boundary as well as temperature and velocity show high deviation from the reference full CFD solution. In particular, average and flow field temperatures show a deviation from the CFD solution up to 25%; average and flow field velocities show a deviation up to 40%. However, if the CFD module is larger than 200 m, average and flow field deviations can be significantly reduced with error of few percents.

3.3. Calculation of the Fan and Fire Characteristic Curves

The adoption of indirect coupling strategies requires the calculation of the characteristic curves of the near field regions. Several runs of the near field CFD model are conducted, varying the pressure difference across the domain boundaries. The results are presented in terms of bulk flow velocity versus total pressure difference. Figure 11 shows the characteristic curve of a single and a pair of operating jet fans. The curves describe the capability of jet fans to produce thrust and they are calculated adopting the methodology presented in [20]. The approach is based on the hypothesis that a series of operating jet fans produces a flow field characterized by a periodic pattern. Therefore, the upstream and downstream boundaries have been defined as periodic surfaces. The hypothesis is confirmed to be valid using CFD simulation of a train of operating jet fans as it is shown in Figure 13.

The same approach has been followed to calculate the characteristic curves of the fire region. Different simulations have been conducted varying the total pressure difference across the domain and calculating the resulting bulk flow velocity.

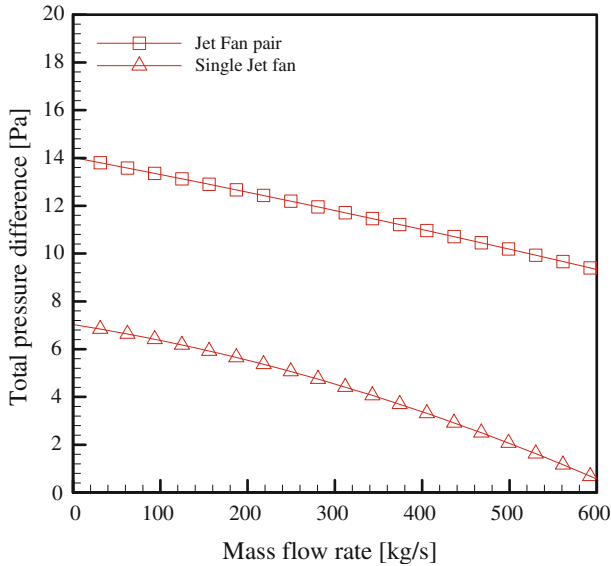


Figure 11. Characteristic curves of a tunnel region 50 m long where an activated jet fan pair (and a single jet fan) is located: pressure drop between inlet and outlet versus mass flow rate across the inlet (CFD calculated).

Figure 12 shows the resulting curves for different fire sizes in the range from 10 MW to 100 MW. The sensitivity of the results to the assumed temperature of the hot gases leaving the top surface of the fire source has been investigated in the experimentally measured range from 1100 K to 1500 K. Despite the temperature difference of 400 K (almost 50% increment), the effect on the curve for the 10 MW scenario is negligible ($\sim 1\%$). For the 30 MW and 50 MW scenarios the effect is smaller than 5%, and for the 100 MW it is smaller than 7%. This relatively small sensitivity is a point in favour of the simplified representation of the fire.

4. Results

4.1. Cold-Flow Scenarios

Multiscale and full CFD models have been used to estimate the performance of the ventilation system in case of cold flow (scenarios without a fire) for different combinations of operating jet fan pairs. Figure 13 shows the flow pattern established for five jet fans pairs operating at the same time. The flow field, calculated using the full CFD model, shows a clear periodic behaviour as evident from the shape of the velocity iso-contours. The multiscale calculations have been conducted using indirect coupling with the jet fan characteristics curves implemented in the 1D model. The multiscale and full CFD predictions of the bulk flow in the

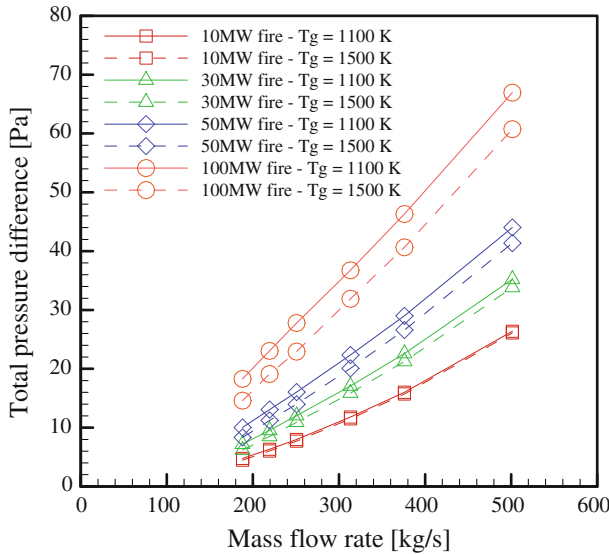


Figure 12. Characteristic curves of the tunnel region 400 m long where the fire is located: pressure drop between inlet and outlet versus mass flow rate across the inlet (CFD calculated).

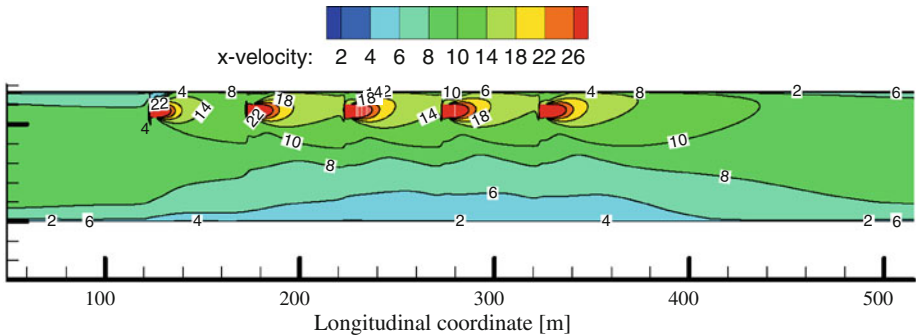


Figure 13. Longitudinal velocity iso-contours, calculated using full CFD, for 10 operating jet fans pairs. (Not to scale).

tunnel as function of the number of operating jet fans are shown in Figure 14. It is seen that the adoption of the multiscale model, including the periodic flow hypothesis, induces a numerical error lower than 1.5% in all scenarios. In Figure 14, two different ventilation scenarios with five operating jet fans pairs have been considered. The first configuration uses all the north portal jet fans while the second uses all the south portal jet fans (see the configuration of the ventilation system as depicted in Figure 4).

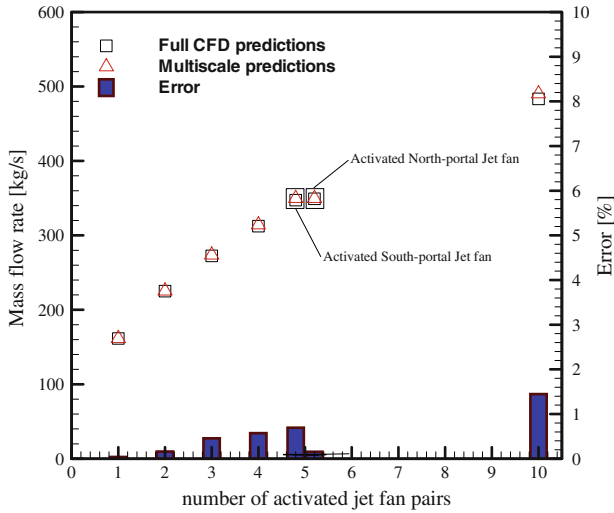


Figure 14. Predictions of average velocity for cold flow scenarios. Comparison and error between multiscale and full CFD results.

The computational time required to run the full CFD model ranged between 48 h and 72 h. The multiscale model with indirect coupling runs almost instantaneously (few seconds).

4.2. Fire Scenarios

Full CFD model and multiscale model with direct and indirect coupling have been used to investigate the performance of ventilation system in case of fire with size ranging from 10 MW to 100 MW. Based on the boundary independence study, the near field of the fire region was set to a length of 400 m. The description of the ventilation strategies and the results are given in Table 2.

The first scenario involves three jet fan pairs operating close to the north portal. This is the minimum number of fans required to guarantee velocities above the critical value for a 30 MW fire. The error for both coupling strategies is very small, below 3.5%. Figure 15 shows the temperature and velocity fields computed with direct coupling for scenario 1. The multiscale model predictions compare very well to the full CFD predictions. In particular no appreciable differences are observed in the temperature field. Very small differences are observed in the longitudinal velocity field. These small differences are due to the presence of the discharge cone generated by the operating jet fans upstream of the fire source which are included in the full CFD representation.

The same conclusions are reached when analyzing the results for scenarios 2–4. The differences in the predicted flow rate range between 0.01% and 1.4% for the direct coupling, and between 0.3% and 2.3% for indirect coupling (see Appendix C for comparison of field results). These results confirm the high accuracy that can be achieved by using a multiscale model. Furthermore, it must be stressed

Table 2
Comparison of the Results from Two Coupling Strategies for Multiscale Modelling and Full CFD for a Wide Range of Fire Sizes and Ventilation Scenarios

Scenario	Fire size	Jet fan						Full scale CFD		Multiscale direct		Multiscale indirect	
		pairs #1-2	pair #3	pair #4	pair #5	Jet fan pairs #6-10	Mass flow rate [kg/s]	Mass flow rate [kg/s]	Mass flow rate [kg/s]	Deviation [%]	Mass flow rate [kg/s]	Deviation [%]	
Scenario 1	30 MW	x	x	-	-	-	-	216.10	220.62	2.09	223.53	3.44	
Scenario 2	30 MW	x	x	x	x	-	301.42	301.44	0.01	305.58	1.38		
Scenario 3	30 MW	x	x	x	x	x	435.19	434.54	0.15	445.52	2.37		
Scenario 4	30 MW	-	-	-	-	x	299.29	296.05	1.08	300.25	0.32		
Scenario 5	10 MW	x	-	-	-	-	204.52	204.48	3.12	197.70	3.33		
Scenario 6	50 MW	x	x	x	-	-	227.19	234.28	0.02	242.74	6.85		
Scenario 7	100 MW	x	x	x	x	-	194.28	208.62	7.38	203.01	4.50		

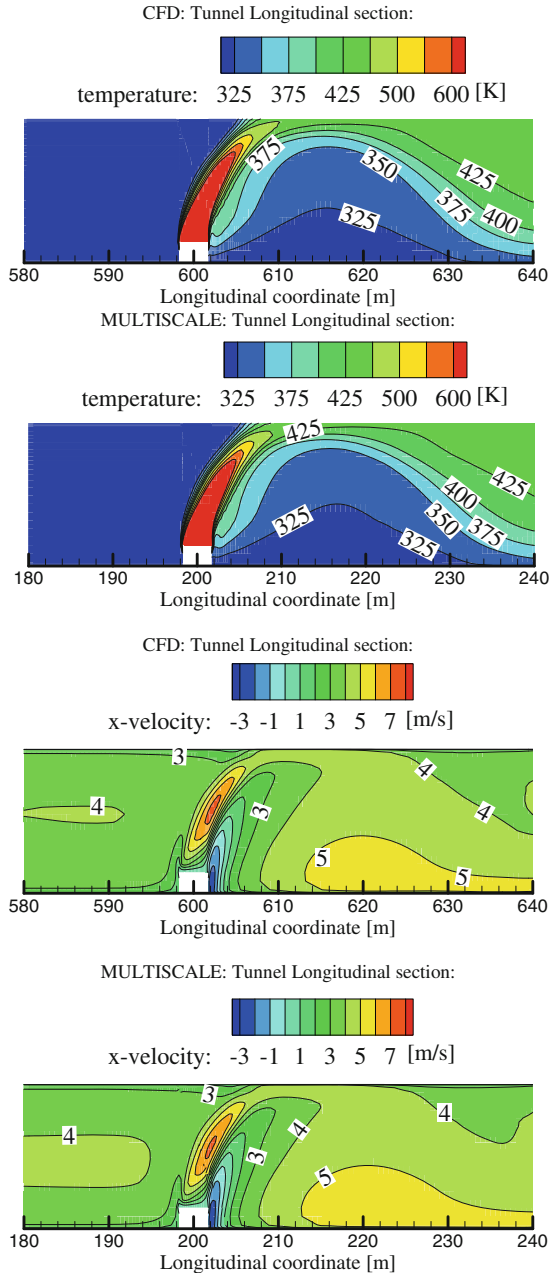


Figure 15. Comparison of results near the fire for the multiscale and the full CFD simulations for a fire of 30 MW and ventilation scenario 1. Velocity and temperature values are expressed in m/s and K, respectively. The longitudinal coordinates start at the upstream boundary of the corresponding CFD domain.

that the simulations of tunnel ventilation flows suffer of high uncertainty on the real boundary conditions at the portals, effective wall roughness, fire load and its geometry, and throttling effects of vehicles. For these reasons, the largest error induced by using the multiscale model is by far within the uncertainty range of the enforced boundary conditions and it is acceptable. On the other hand, the significantly lower computational time required by the multiscale methodology (2 h for the direct coupling, few seconds for the indirect coupling against the 48 h to 72 h for the full CFD model) is of great advantage because several ventilation scenarios can be explored and extensive sensitive analysis and parametric studies can be conducted.

Table 2 also shows that the number of operating jet fans required to achieve critical ventilation velocity in the fire region varies with the fire size. In particular 2, 4 and 5 jet fan pairs must be activated to provide super-critical ventilation velocity for a 10 MW, 50 MW and 100 MW fire, respectively. These results show that the fire throttling effect is large.

Comparing the effect of the number of operating jet fans in cold flow scenarios (Figure 14) to the fire scenarios (Table 2), the fire throttling effect can be quantified. For a 100 MW fire, the mass flow when five jet fan pairs are activated is ~ 200 kg/s. When five jet fan pairs are activated in cold flow scenario, the flow is ~ 290 kg/s. Thus, the effect of the 100 MW is to decrease the ventilation flow by more 30%. The analysis presented shows that the fire throttling effect is large and must be taken into account in tunnel flow calculations. This phenomenon was already observed experimentally in 1979 [36].

In this work, the ventilation scenarios are set for super-critical velocities preventing smoke back-layering. Thus, the assumption of 1D flow at the upstream boundary is guaranteed. In order to use the multiscale model to investigate sub-critical ventilation scenarios, the upstream boundary must be moved to ensure that all the back-layering is captured within the CFD domain. If otherwise, the results will be dependent on the length of the 3D domain. A rough estimation of the back-layering distance to properly design the dimension of the CFD zone for sub-critical ventilation scenarios can be obtained using the experimental correlation presented in [37]. However, great care must be adopted as the correlation is based on small scale experimental data. A posteriori post-processing of the CFD results must always be conducted to clarify this matter.

5. Concluding Remarks

A novel and fast modelling approach is applied to simulate tunnel ventilation flows during fires. The technique is based on the evidence that there are very long tunnel regions where the flow is fully developed (*far field*), and relatively short portions showing 3D flow conditions (*near field*). The multiscale methodology uses different levels of computational sophistication to model each tunnel region saving computational time without decreasing the numerical accuracy. In particu-

lar, the far field is modelled using a 1D model and the near field using a CFD model.

Both direct and indirect coupling strategies are used and compared for steady state conditions. The methodology has been applied to a modern tunnel with 53 m² cross section and 1.2 km in length. Different fire scenarios ranging from 10 MW to 100 MW are investigated with a varying number of operating jet fans. The effects of the mesh size and location of the 1D–3D interfaces have also been investigated.

It is shown that the accuracy of the multiscale model is high when compared to the full CFD solution. In particular, the error for all the studied scenarios is below few percents. The small numerical error is more than acceptable when compared to the large uncertainty of the real meteorological conditions at the portals, actual fire load, effective lining roughness, presence of vehicles and obstructions, etc.

To the best knowledge of the authors, this is the first time that a ventilation system has been coupled to a fire. This has allowed, among other things, to quantify the fire throttling effect, which is seen to be large and to reduce the flow up to 30% for a 100 MW fire.

The multiscale model has been demonstrated to be a valid technique for the simulation of complex tunnel ventilation systems. It can be successfully adopted to conduct parametric and sensitivity studies, to design ventilation systems, to assess system redundancy and to assess the performance under different hazards conditions. Furthermore, the authors believe that the multiscale methodology represents the only feasible tool to conduct accurate simulations in tunnels longer than few kilometres, when the limitation of the computational cost becomes too restrictive.

Acknowledgements

The authors would like to thank Dr Vittorio Verda and Dr Ricky Carvel for their help and the interesting discussions on the subject permitting the publication of this paper.

Appendix A: Additional Grid Independence Plots

Some of the temperature and velocity contours calculated in the grid independence study are presented in Figure 16. It shows the contours of temperature and horizontal velocity at Reference Section 2 located 100 m downstream the fire source. They are computed for four difference meshes whose characteristics are summarized in Sect. 3.1. As expected from the previous results, the computed solutions show larger deviations for the courses meshes 1 and 2 while convergence is obtained for finer meshes 3 and 4.

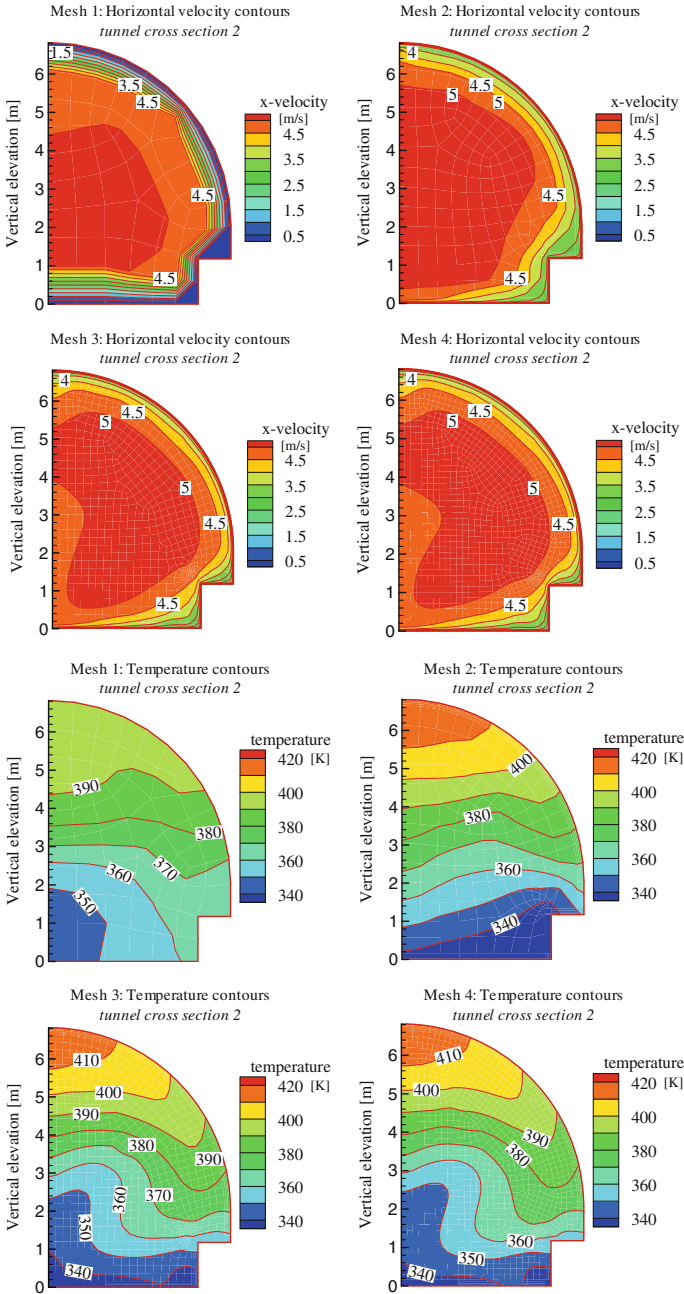


Figure 16. Comparison of the longitudinal velocity (left) and temperature (right) contours for meshes #1 to #4 in the tunnel Reference Section 2 for a 30 MW fire. Velocity and temperature values are expressed in m/s and K, respectively.

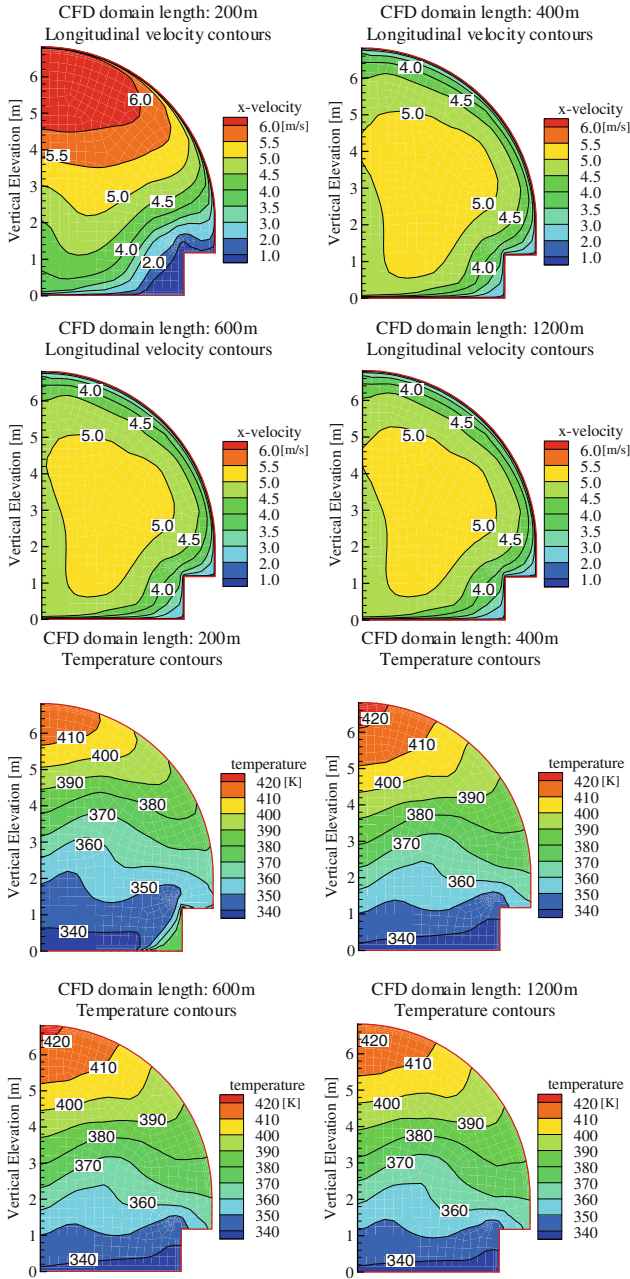


Figure 17. Effect of the CFD domain length L_{CFD} on the horizontal velocity and temperature fields at Reference Section 2 for a 30 MW fire. Velocity and temperature values are expressed in m/s and K, respectively.

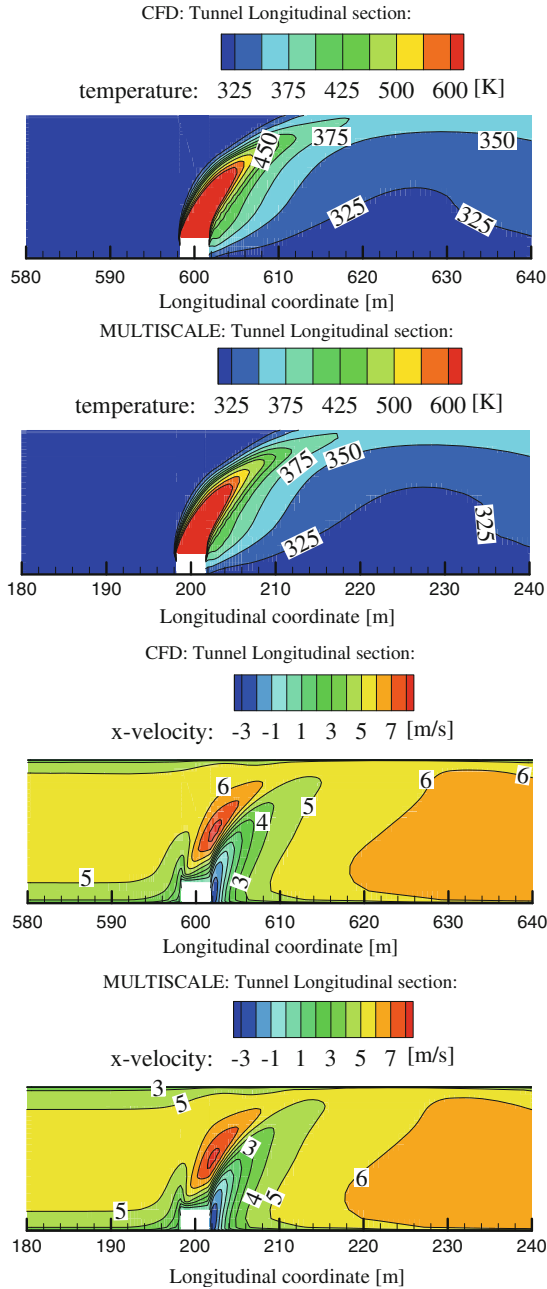


Figure 18. Comparison of results near the fire for the multiscale and the full CFD simulations for a fire of 30 MW and ventilation scenario 2. Velocity and temperature values are expressed in m/s and K, respectively. The longitudinal coordinates start at the upstream boundary of the corresponding CFD domain.

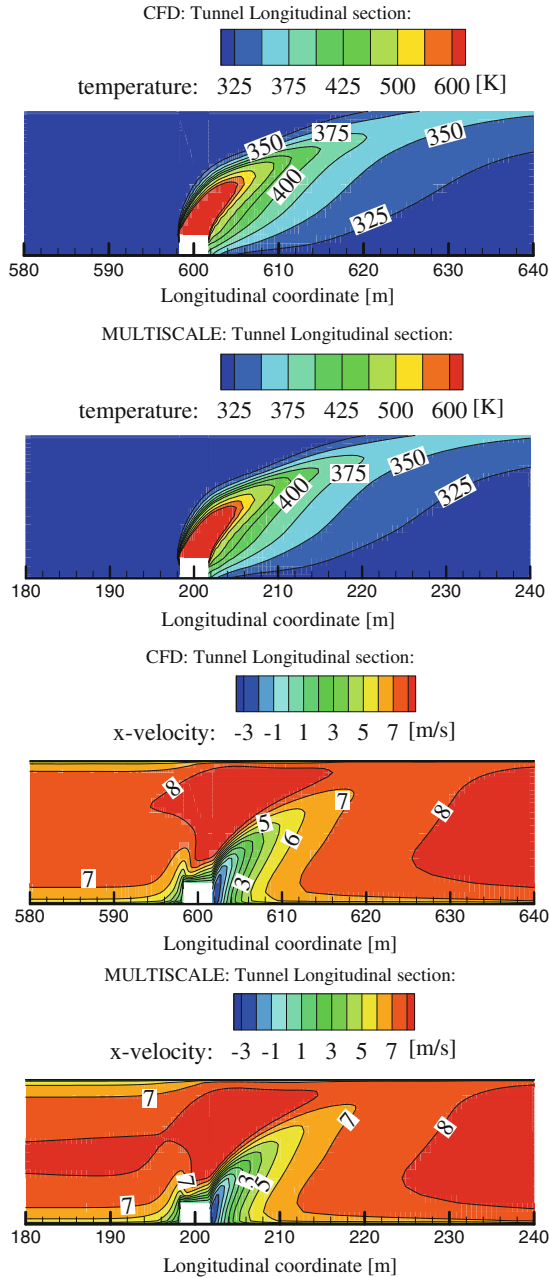


Figure 19. Comparison of results near the fire for the multiscale and the full CFD simulations for a fire of 30 MW and ventilation scenario 3. Velocity and temperature values are expressed in m/s and K, respectively. The longitudinal coordinates start at the upstream boundary of the corresponding CFD domain.

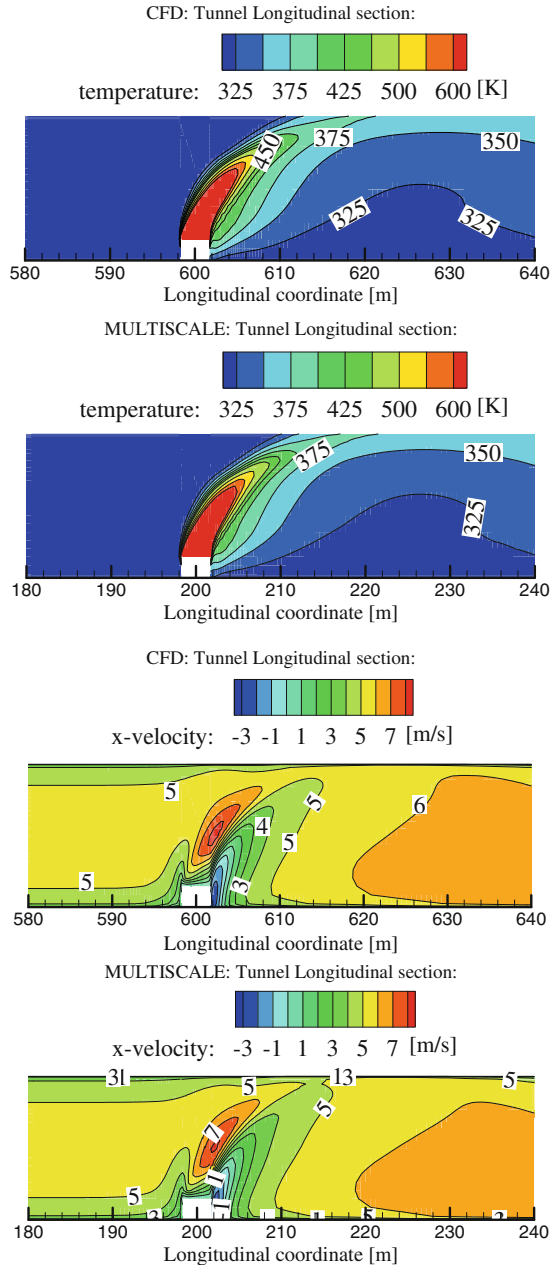


Figure 20. Comparison of results near the fire for the multiscale and the full CFD simulations for a fire of 30 MW and ventilation scenario 4. Velocity and temperature values are expressed in m/s and K, respectively. The longitudinal coordinates start at the upstream boundary of the corresponding CFD domain.

Appendix B: Additional Boundary Independence Plots

The results of the boundary independence study relative to the tunnel Reference Section 2, located 100 m downstream the fire are presented in Figure 17. Also in this case, the analysis of the temperature and velocity fields shows that highly accurate results can be achieved with 3D domains whose downstream boundary is at a minimum distance of 100 m from the furthest location where a CFD accurate solution is required.

Appendix C: Scenarios 2–4—Comparison of the Field Results for Multiscale and Full CFD Representations

Additional results on the temperature and velocity fields computed using multiscale and full CFD techniques are presented here. They include the ventilation scenarios 2–4 (see Figures 18, 19 and 20). These field data also confirm that high numerical accuracy can be achieved by using a multiscale technique.

References

1. Carvel R (2007) Tunnel fire safety systems. *EuroTransp* 5(6):39–43
2. Ferro V, Borchiellini R, Giaretto V (1991) Description and application of tunnel simulation model. Proceedings of aerodynamics and ventilation of vehicle tunnels conference, pp 487–512
3. Jacques E (1991) Numerical simulation of complex road tunnels. Proceedings of aerodynamics and ventilation of vehicle tunnels conference, pp 467–486
4. Riess I, Bettelini M, Brandt R (2000) SPRINT—a design tool for fire ventilation. Proceedings of aerodynamics and ventilation of vehicle tunnels conference
5. Cheng LH, Ueng TH, Liu CW (2001) Simulation of ventilation and fire in the underground facilities. *Fire Saf J* 36(6):597–619
6. Jang H, Chen F (2002) On the determination of the aerodynamic coefficients of highway tunnels. *J Wind Eng Indus Aerodyn* 89(8):869–896
7. Dai G, Vardy AE (1994) Tunnel temperature control by ventilation. Proceedings of 8th international symposium on the aerodynamics and ventilation of vehicle tunnels, Liverpool, UK, 6/8 July, pp 175–198
8. William D. Kennedy (1997) Critical velocity—past, present and future (revised 6 June 1997). American public transportation association's rail trail conference in Washington, DC
9. Wang L, Haworth DC, Turns SR, Modest MF (2005) Interactions among soot, thermal radiation, and NO_x emissions in oxygen-enriched turbulent non-premixed flames: a computational fluid dynamics modelling study. *Combust Flame* 141:170–179
10. Woodburn PJ, Britter RE (1996) CFD simulation of tunnel fire—part I. *Fire Saf J* 26:35–62
11. Woodburn PJ, Britter RE (1996) CFD simulation of tunnel fire—part II. *Fire Saf J* 26:63–90
12. Wu Y, Bakar MZA (2000) Control of smoke flow in tunnel fires using longitudinal ventilation systems—a study of the critical velocity. *Fire Saf J* 35:363–390
13. Vauquelin O, Wu Y (2006) Influence of tunnel width on longitudinal smoke control. *Fire Saf J* 41:420–426

14. Van Maele K, Merci B (2008) Application of RANS and LES field simulations to predict the critical ventilation velocity in longitudinally ventilated horizontal tunnels. *Fire Saf J* 43:598–609
15. Armstrong J (1993) The ventilation of vehicle tunnels by jet fans—the axisymmetric case. Proceedings of the seminar on installation effects in fan systems. Mechanical Engineering Press, London
16. Tabarra M (1995) Optimizing jet fan performance in longitudinally ventilated rectangular tunnels. Separated and complex flows. *ASME FED* 217:35–42
17. Karki KC, Patankar SV (2000) CFD model for jet fan ventilation systems. Proceedings of aerodynamics and ventilation of vehicle tunnels conference
18. Massachusetts Highway Department (1995) Memorial tunnel fire ventilation test program comprehensive test report
19. Galdo Vega M, Arguelles Diaz KM, Fernandez Oro JM, Ballesteros Tajadura R, Santolaria Morros C (2008) Numerical 3D simulation of a longitudinal ventilation system: memorial tunnel case. *Tunn Undergr Space Technol* 23(5):539–551
20. Colella F, Rein G, Borchiellini R, Carvel R, Torero JL, Verda V (2009) Calculation and design of tunnel ventilation systems using a two-scale modelling approach. *Build Environ* 44:2357–2367. doi:10.1016/j.buildenv.2009.03.020
21. Fox RW, McDonald AT (1995) Introduction to fluid mechanics, 4th edn. John Wiley and Sons, Singapore
22. Gutiérrez-Montes C, Sanmiguel-Rojas E, Kaiser AS, Viedma A (2008) Numerical model and validation experiments of atrium enclosure fire in a new fire test facility. *Build Environ* 43:1912–1928
23. Launder BE, Spalding DB (1974) The numerical computation of turbulent flows. *Comput Methods Appl Mech Eng* 3(2):269–289
24. Versteeg HK, Malalasekera W (2007) An introduction to computational fluid dynamics, the finite volume method, 2nd edn. Pearson Prentice Hall, Glasgow
25. Lacasse D, Turgeon E, Pelletier D (2004) On the judicious use of the k-3 model, wall function and adaptivity. *Int J Therm Sci* 43(10):925–938
26. Schlichting H (1979) Boundary layer theory, 7th edn. McGraw-hill, New York
27. Cox G, Kumar S (2002) Modelling enclosure fires using CFD. In: *The SFPE handbook for fire safety engineering*, 3rd edn. NFPA, Massachusetts International, Quincy
28. Lonnemark A, Ingason H (2005) Gas temperature in heavy goods vehicles fires in tunnels. *Fire Saf J* 40:506–527
29. Heskestad G (2002) Fire plumes, flame height and air entrainment. In: *The SFPE handbook for fire safety engineering*, 3rd edn. NFPA, Massachusetts International, Quincy
30. Loennermark A, Ingason H (2008) The influence of tunnel cross-section on temperature and fire development, 3rd International symposium on tunnel safety and security, Stockholm, Sweden, March 12–14
31. Ingason H (2008) Model scale tunnel tests with water spray. *Fire Saf J* 43:512–528
32. Drysdale D (2000) An introduction to fire dynamics II edition. John Wiley & Sons Inc, Hoboken, USA
33. Reszka P, Steinhaus T, Biteau H, Carvel RO, Rein G, Torero JL (2007) A Study of fire durability for a road tunnel comparing CFD and simple analytical models. EURO-TUN07 computational methods in tunnelling, Wien. <http://hdl.handle.net/1842/1892>
34. Kunsch JP (2002) Simple model for control of fire gases in a ventilated tunnel. *Fire Saf J* 37(1):67–81
35. Oka Y, Atkinson GT (1995) Control of smoke flow in tunnel fires. *Fire Saf J* 25(4):305–322

36. Lee CK, Chaiken RF, Singer JM (1979) Interaction between duct fires and ventilation flow: an experimental study. *Combust Sci Technol* 20:59–72
37. Ingason H (2005) Fire Dynamics in tunnel. In: Beard A, Carvel R (eds) *The handbook of tunnel fire safety*. Thomas Telford, London, UK